JOURNAL OF THERMOPHYSICS AND HEAT TRANSFER
Vol. 19, No. 1, January–March 2005

Impingement Heat Transfer, Part I: Linearly Stretched Arrays of Holes

Lujia Gao* and Srinath V. Ekkad†
Louisiana State University, Baton Rouge, Louisiana 70803
and
Ronald S. Bunker‡
General Electric Global Research and Development Center, Niskayuna, New York 12309

This is Part I of a two-part paper to study new configurations for impingement heat transfer. In Part I, linearly stretched arrays of holes are investigated, and in Part II the effect of pressure gradient on jet-impingement heat transfer is studied. Impingement holes in real engines are primarily directed to hot spot locations, thus producing nonsquare arrays. In this study, the spacing between the holes increases in both the streamwise and spanwise direction simulating the stretching of the hole arrays downstream. Two different arrays are investigated with the first array having uniform diameter holes through the array placed in a stretched format and the second array having increasing diameter holes. Three jet Reynolds numbers between 2×10^3 and 10^3 are studied for three different jet height-to-diameter ratios between 1 and 5. The measured heat-transfer coefficients for these arrays are then predicted using existing impingement heat-transfer correlations based on regular evenly spaced arrays. Results show that the published correlations overpredict the effect of crossflow by about 20–40% and show stronger heat-transfer degradation for the downstream rows. Also, the correlation was extrapolated for this study as a result of the lack of information for extremely strong crossflow effects. All measurements were obtained using the transient liquid crystal technique.

Nomenclature

A	=	constant in Florschuetz et al. correlation[5]
B	=	constant in Florschuetz et al. correlation[5]
D	=	impingement jet hole diameter (0.635 cm)
G	=	mass flux, kg/m$^2 \cdot$ s
h	=	local convection heat-transfer coefficient, W/m$^2 \cdot$ K
k	=	thermal conductivity of Plexiglas® surface, W/m $\cdot$ K
k_{air}	=	thermal conductivity of air, W/m $\cdot$ K
Nu	=	Nusselt number, hD/k_{air}
Pr	=	Prandtl number, ν/α
Re	=	Reynolds number, $\rho V_j D/\mu$
T_i	=	initial temperature of test section, K
T_m	=	mainstream temperature of the flow, K
T_w	=	color-change temperature of the liquid crystal (red-to-green), K
t	=	time of liquid crystal color change, s
UD	=	uniform diameter array
V_j	=	average jet velocity, m/s
VD	=	variable diameter array
X	=	streamwise distance of the impingement surface (exit flow direction), m
Y	=	spanwise distance on the impingement surface, m
Z	=	jet hole-to-target wall spacing, also H, m
α	=	thermal diffusivity of Plexiglas, m^2/s
μ	=	fluid dynamic viscosity, kg/(m $\cdot$ s)
ν	=	kinematic viscosity, m^2/s
τ	=	time step
ϕ	=	crossflow coefficient from Kercher and Tabakoff

Subscripts

c	=	crossflow
j	=	jet

Received 24 February 2004; revision received 28 June 2004; accepted for publication 28 June 2004.

*Graduate Research Assistant, Mechanical Engineering Department.
†Associate Professor, Mechanical Engineering Department. Member AIAA.
‡Senior Scientist. Member AIAA.

Introduction

IMPINGEMENT jet arrays are widely used as a heat-transfer enhancement method for cooling or heating purposes. This scheme is used extensively in gas turbine systems as a result of the high heat-transfer capabilities of the jet. Typically, the jets are in arrays, and the arrangement of the arrays is determined based on cooling requirements on the airfoil or shroud surfaces. The arrays are not always in the square form where the jet-to-jet spacing is evenly distributed along the surface. Also, the jet-to-impingement surface distance varies at different locations. This is typically a regular array of holes that can appear stretched in the streamwise and spanwise direction, resulting in increased spacing for the downstream holes. Their use is essentially to increase surface cooling coverage, where arrays are tailored or varied according to the external heat loading. This method is not only used to produce distributed cooling on hot surfaces to increase overall effectiveness with limited coolant usage but also to counteract the effects of crossflow degradation, which could be severe if the array is stretched. These liner stretched arrays have been an issue for backside cooling for dry low emission (DLE) combustor liners.

Previous studies on jet-impingement heat transfer[1–7] summarized findings relating to parametric effects of jet geometry, temperature, crossflow, turbulence, etc. on impingement heat and mass transfer. Kercher and Tabakoff[2] and Florschuetz et al.[5] determined that the heat-transfer characteristics for jet array impingement are affected by the crossflow. They presented correlations for both inline and staggered hole patterns including effects of crossflow on impingement heat transfer. A comprehensive literature survey of all of the jet-impingement studies and the correlations are summarized by Downs and James.[8] Huber and Viskanta[9,10] studied the effect of jet-to-jet spacing and also compared heat transfer for perimeter and center jets in a confined, impinging array of axisymmetric air jets. All of the preceding studies presented the effects of various parameters on jet-impingement heat transfer. Van Treuren et al.[11] were the first to present detailed distributions under impinging jets. They measured

both local heat-transfer coefficient and adiabatic wall temperature under the impinging jets. Huang et al.[12] studied the effect of crossflow direction on impingement heat transfer for a square array of jet holes. They investigated only one jet-to-wall distance. They indicated that the crossflow effect is minimal when the flow exits in both directions after impingement. Recently, Bailey and Bunker[13] studied the effect of jet array geometry by varying the spacing in a square array that looked at arrays of spacing $(X/D \times Y/D)$ 3×3, 6×6, and 9×9. They also varied the jet plate-to-target wall distance ratio Z/D from 1.25 to 5.5. They presented a modified correlation to accommodate their new results provided by Florschuetz et al.[5] Ekkad et al.[14] presented heat-transfer distributions for in-line square arrays of spacing 4×4, 8×8, and rectangular arrays of spacing of four in the streamwise direction and eight in the spanwise direction. They also varied their jet-to-wall spacing H/D from 1 to 5. They clearly showed that closer spacing increases the jet-to-jet interaction and produces higher heat transfer in the regions between jets.

Detailed heat-transfer coefficient distributions are presented for impingement arrays that are linearly stretched. Two different arrays have been investigated, one with uniform diameter holes and one with varying diameter holes for each row. The effect of Reynolds number and jet hole-to-target plate distance was also investigated. The main goal is to make actual measurements for stretched arrays and compare the results to predictions based on correlations developed by Kercher and Tabakoff[2] and Florschuetz et al.[5] The linearly stretched arrays were chosen as the simplest example for comparing with existing correlations. The goal is not to compare the two stretched arrays but to compare the predictions from existing correlations to different stretched array configurations. Chance[3] also provides a jet-impingement correlation with crossflow effects. However, we have not compared with that correlation because Ref. 2 uses similar equations as Ref. 3. The transient liquid crystal technique is a very established technique for detailed heat-transfer measurements. Ekkad and Han[15] presented a detailed description of the technique and its applications to various heat-transfer problems. They also provided a detailed uncertainty analysis and reliability of the technique when applied to different situations. Because of redundancy issues, the technique is not discussed in detail in this study.

Test Description and Apparatus

Figure 1 shows the entire test setup. The compressed air supply is passed through an orifice meter to measure the mass flow rate entering the test section. This mass flow rate is set to produce the effective jet Reynolds number. The flow is then heated through an inline air heater, where the exit temperature is controlled through a solid-state relay-based temperature controller. The air is bypassed away from the test section through a three-way diverter valve during the heating. When the air reaches a steady temperature, the transient test is initiated by flipping the valve, and the hot air is routed into the test section. The time counter on the image processing system takes a 2–4 s lag to allow for flow to reach the impingement plate. The time lag changes with the set Reynolds number of the flow. The inside wall or the impingement wall of the test surface is coated with a thin layer of thermochromic liquid crystals (R35C1W). The initial red color appears at 35°C, the green appears at 35.4°C, and the blue appears at 36°C. A black paint layer (~5 μm) is coated on top of the liquid crystal paint to ensure that the colors are visible through the Plexiglas® wall. The image processing system consists of an red/green/blue (RGB) camera to view the liquid crystal coated impingement surface during the transient heating test and a color frame grabber board embedded in the PC slot. The frame grabber board is programmed to analyze the color changes. The time of transition of the liquid crystals from colorless to green at each point on the test surface during the transient test is recorded at every pixel on the test surface. The air temperature before the flow enters the jet plate is measured using the data-acquisition system. There are three thermocouples to measure the variation of the channel temperature before impingement to monitor proper mixing of the flow in the chamber prior to impingement. These thermocouples are placed just upstream of the jet plate at different span locations to ensure that the temperatures are not varying in the plenum before impingement. One more fast-response thermocouple (32-gauge) is placed at the entrance to a hole in the middle of the array. This thermocouple measures the mainstream temperature with respect to time during the experiment. The velocity of the air is significant inside the hole to provide adequate response time for temperature measurement during the transient test.

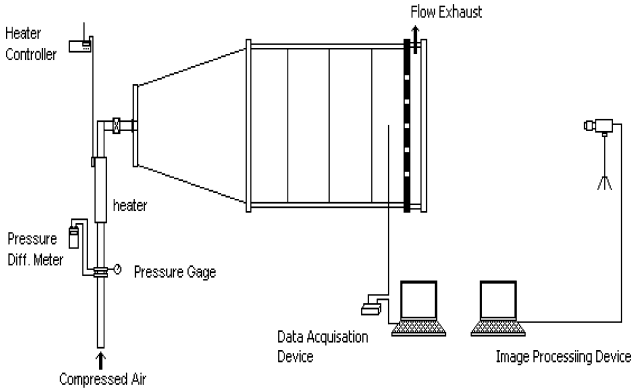

Fig. 1 Schematic of the experimental setup.

The test section is a 38.1×38.1 cm square cross-section channel. The air enters the test section through a 2.54-cm pipe and is expanded into the 38.1-cm-square area through a diffuser piece. The flow is then passed through three plastic screens to enable mixing and reducing the turbulence of the incoming flow. The flow then enters the test section area through a jet plate. The area increase before jet impingement reduces flow velocity to less than 0.2 m/s. The thickness of the jet plate is 1.27 cm and is made of Plexiglas. The jet-impingement area is closed in three directions, and air exits only in one direction. This direction of exit flow is called flow direction, and the direction orthogonal to it is called spanwise direction.

The jet plate can be easily replaced to change the jet array configuration. Figure 2a shows the uniform diameter jet plate. All of the holes are of a uniform diameter with holes of diameter 0.635 cm. The first row of holes are placed two hole diameters apart from each other in the spanwise direction. The second row of holes are placed three hole diameters apart, and the second row is placed two-hole diameters downstream of the first row. Similarly, the downstream rows are placed in an increasing distance both in spanwise and streamwise direction simulating a stretched array of holes. Figure 2b shows the varying diameter plate. In this case, the hole diameters are increasing from the first row with hole diameters of 0.3175 cm to the last row with 0.635 cm. The locations of the holes are identical on the plate to the uniform diameter holes resulting in varying spanwise and streamwise normalized distances. Table 1 shows the normalized distances comparing the uniform and varying diameter plates. The spacing between the jet plate can be varied by changing the wall spacers along the three closed sides and changing the wall distance-to-jet diameter ratio Z/D. These values are also presented in Table 2.

Table 1 Jet-plate dimensions

Row no.	Hole diameter, cm		Normalized spanwise spacing based on local hole diameter *Y/D*		Normalized streamwise spacing based on upstream hole diameter *X/D*	
	UD	*VD*	*UD*	*VD*	*UD*	*VD*
1	0.635	0.3175	2	4	——	——
2	0.635	0.3630	3	5.25	2	4
3	0.635	0.4082	4	6.22	3	5.25
4	0.635	0.4765	5	6.66	4	6.22
5	0.635	0.4989	6	7.63	5	6.66
6	0.635	0.5443	7	8.17	6	7.63
7	0.635	0.5895	8	8.62	7	8.17
8	0.635	0.635	9	9	8	8.62

Table 2 Jet plate-to-target wall dimensions *H/D*

	Jet-to-wall spacing					
	$H = 0.635$ cm		$H = 1.905$ cm		$H = 3.175$ cm	
Row number	*UD*	*VD*	*UD*	*VD*	*UD*	*VD*
1	1	2	3	6	5	10
2	1	1.75	3	5.25	5	8.25
3	1	1.56	3	4.67	5	7.78
4	1	1.33	3	3.99	5	6.65
5	1	1.27	3	3.82	5	6.36
6	1	1.17	3	3.51	5	5.83
7	1	1.08	3	3.24	5	5.40
8	1	1	3	3	5	5

Procedure and Data Reduction

Details of the experimental procedure are similar to that presented by Huang et al.[12] and Ekkad et al.[14] A one-dimensional transient conduction model into a semi-infinite surface with a convective boundary condition at the surface is assumed.[14,15] The surface temperature response is described by the solution:

$$T_w - T_i = \sum_{j=1}^{N} \left\{ 1 - \exp\left[\frac{h^2\alpha(t-\tau_j)}{k^2}\right] \operatorname{erfc}\left[\frac{h\sqrt{\alpha(t-\tau_j)}}{k}\right] \right\} [\Delta T_{\mathrm{mj}}] \tag{1}$$

The time history of the mainstream temperature is reproduced as a series of step functions using the Duhamel's superposition theorem,

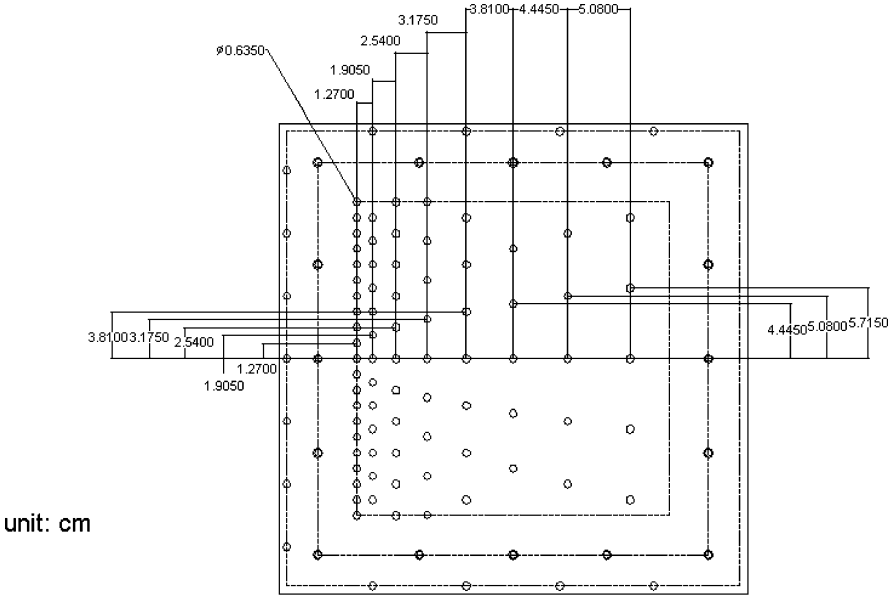

a) Uniform diameter plate

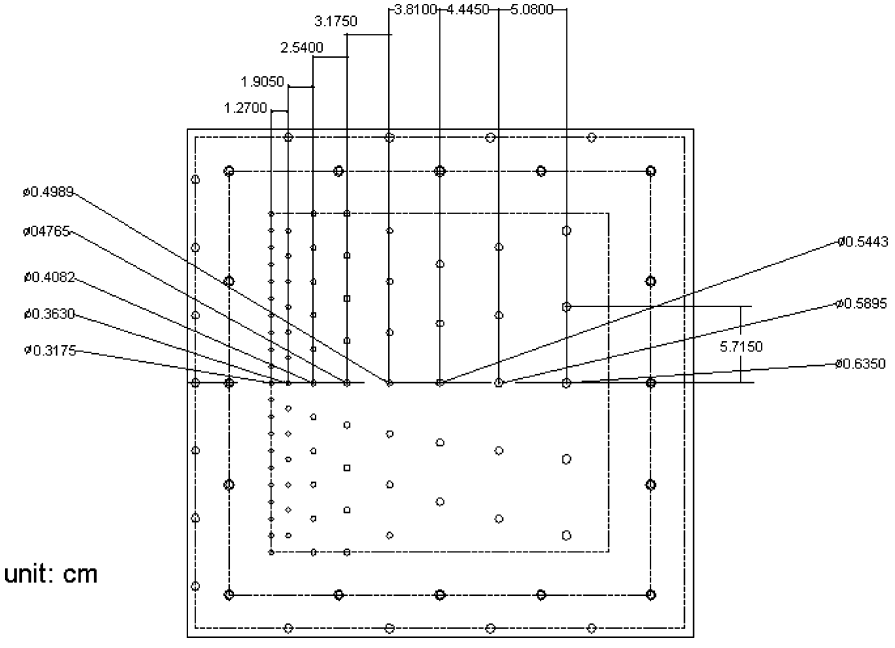

b) Varying diameter plate

Fig. 2 Impingement jet plates.

where ΔT_m and τ_j are the temperature and time step changes from the data-acquisition system output. The equation is solved to obtain the local heat-transfer coefficient at every point on the measured region. More details are presented by Ekkad and Han.[15]

The average uncertainty in heat-transfer coefficient measurement, estimated by the method of Kline and McClintock,[16] is about ±6.9%. The individual uncertainties in the measurement of the time of color change ($\Delta t = \pm 0.5$ s), the mainstream temperature ($\Delta T_m = \pm 1^\circ$C), the color change temperature ($\Delta T_w = \pm 0.2^\circ$C), and the wall material properties ($\Delta\alpha/k^2 = \pm 5\%$). These uncertainties were included in the calculation of the overall uncertainty in the measurement of h. Repeatability tests were run consistently for most cases. Results are repeatable within 3–4% of previous tests. Most of the errors are caused by human and thermocouple errors. The two-dimensional lateral effects are not significant because of the low thermal conductivity of Plexiglas and also the short duration of the test. This has been consistently proved over the past decade in transient liquid crystal studies.[15]

Results and Discussion

The experiments were performed at three different Reynolds numbers of 2×10^3, 6×10^3, and 10^3. The jet Reynolds number is based on average hole diameter and average jet velocity. The average jet velocity was calculated based on the total mass flow rate and the total area of jet holes. For the uniform diameter plate, the uniform diameter and the average diameter are same at 0.635 cm. For the variable diameter, the average diameter is 0.4318 cm. Flow measurements were performed to estimate the amount of mass flow through each row of holes and the amount of crossflow effect on each flow. Figure 3 shows the percent mass flow compared to the total mass flow through each hole and the amount of crossflow at the hole location. Results are presented for both the uniform diameter and varying diameter case. For the uniform diameter case, the number of holes in the first row is highest, resulting in almost 30% of the total flow occurring through the first row. As the number of holes decreases in subsequent rows, the jet flow decreases. The crossflow is significant even for the second row of hole with 30% of total flow becoming crossflow. For the varying diameter case, the jet flow through each row is between 10 and 15% for each of the eight rows of holes showing almost even distribution of mass flow. The crossflow development is also more gradual than for the uniform diameter holes. This flow information is critical towards predicting heat-transfer coefficients from correlations presented by Kercher and Tabakoff[2] and Florschuetz et al.[5] The flow distribution is also valid for all Z/D spacings as the pressure differences between first row to exit of the impingement channel show minimum variations with changes in Z/D.

Figure 4 presents the local jet Reynolds variation for both uniform and varying diameter rows. The uniform diameter jet Reynolds numbers are constant as the hole diameters and jet velocities are constant. For the uniform hole diameters, the jet velocities are almost identical, but the hole diameters increase downstream resulting in higher Reynolds numbers. These local Reynolds numbers were used to compute the heat-transfer coefficients while using the correlations from previous studies.[2,5]

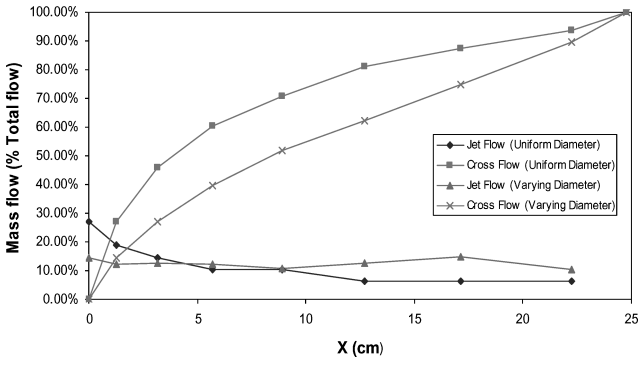

Fig. 3 Jet flow and crossflow distributions for both jet plates.

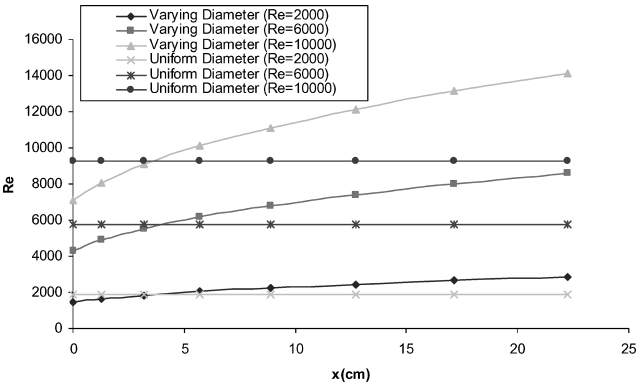

Fig. 4 Jet Reynolds-number variation based on row location and local hole diameter.

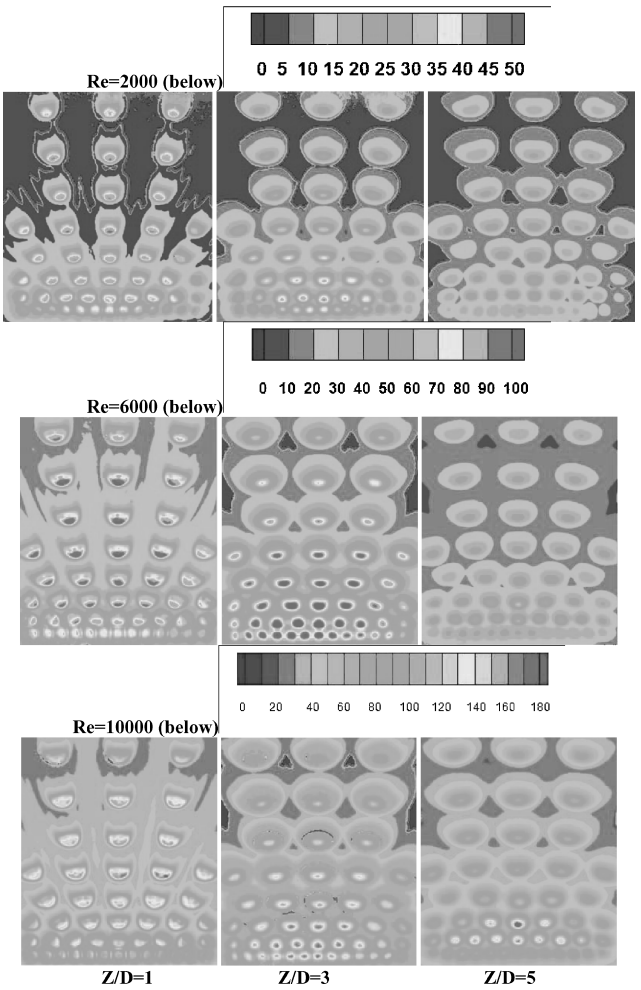

Fig. 5 Detailed Nusselt-number distributions for uniform diameter jet plates.

Uniform Diameter Cases

Figure 5 presents the detailed Nusselt-number distributions for the uniform diameter cases. The local heat-transfer coefficients are normalized by the hole diameter (1.27 cm). The streamwise flow is from bottom to top. The effect of Reynolds number and jet height is presented. It appears that the interaction between the jets decreases downstream as the jets become sparse from first row to the eighth row of holes. The jets also appear to be spreading outward with an increase heat-transfer coefficients in between the holes. The crossflow effect is also evident with the widened heat-transfer zone behind the impingement locations. The crossflow effect seems strongest for the

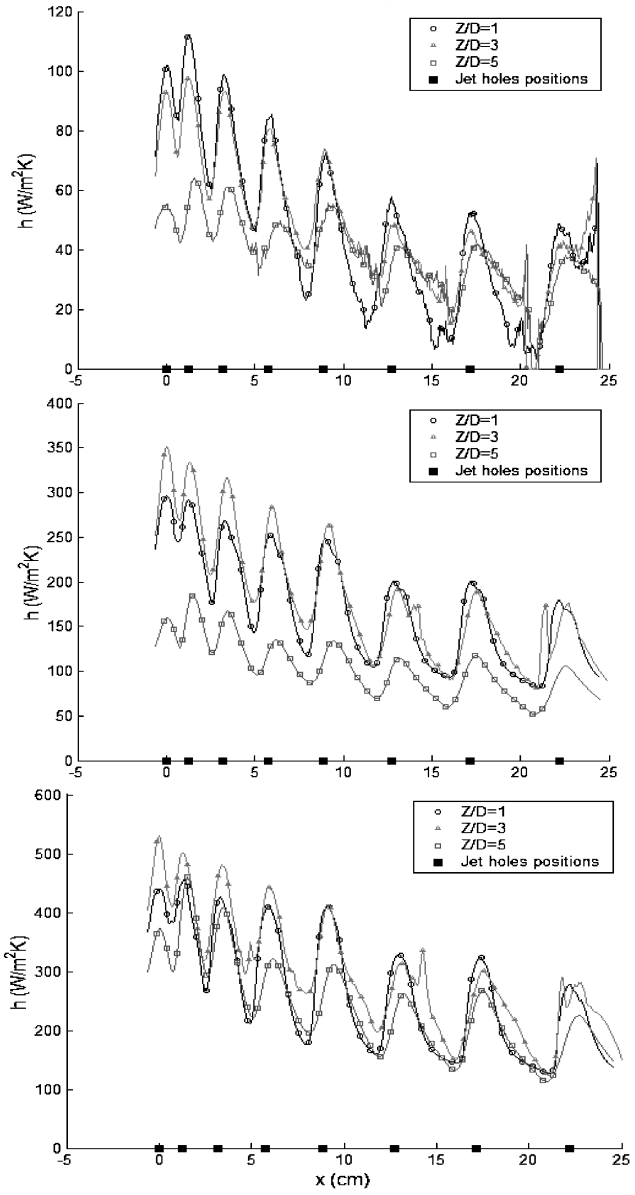

Fig. 6 Effect of jet height on span-averaged heat-transfer coefficients for uniform diameter jet plate: top, $Re = 2 \times 10^3$; middle, $Re = 6 \times 10^3$; bottom, $Re = 10^3$.

jet height-to-target wall Z/D ratio of 1.0. A Z/D of 3.0 produces the highest heat-transfer coefficients compared to the other Z/D ratios for this geometry. The detailed heat-transfer coefficient distributions clearly show that the tendency of increased crossflow is to push the jets away from the wall, resulting in lower heat-transfer coefficients directly underneath the impinging jets.

Figure 6 presents the span-averaged heat-transfer coefficient distributions ($W/m^2 \cdot K$) for each Reynolds number comparing the effect of jet height-to-wall ratio Z/D. The heat-transfer coefficients are plotted against actual distance in centimeters. For a $Re = 2 \times 10^3$, the heat-transfer coefficients for $Z/D = 1$ and 3 are high for the upstream rows. However, the heat-transfer coefficients decrease rapidly further downstream. However for $Z/D = 5$, the heat-transfer coefficients for each row appear to be periodic with slight degradation for the downstream holes. For the seventh and eighth rows, all three heights produce similar levels of heat-transfer coefficients. For $Re = 6 \times 10^3$, the $Z/D = 3$ case clearly produces higher heat-transfer coefficients compared to $Z/D = 1$ and 5. However for $Z/D = 1$, the levels of heat-transfer coefficient for the downstream rows are comparable to that for $Z/D = 3$. At $Re = 10^3$, all three cases show similar levels of heat-transfer coefficient. The peaks are stronger for $Z/D = 1$ and 3, but the valleys are flatter for $Z/D = 5$.

Varying Diameter Cases

Figure 7 presents the detailed Nusselt-number distributions for the varying diameter cases. Again, the normalization diameter was chosen as 1.27 cm, which is the size of the largest hole placed in the last row of this array to be consistent with the Reynolds-number calculation as stated for uniform diameter cases. The exit flow direction is from the bottom to the top of the page. The trends are similar with jet impingement strong for the upstream holes and decreasing downstream with increasing crossflow effects. It appears that the heat-transfer coefficients underneath the impingement holes are much higher for this geometry than for the uniform diameter holes. Also, the jet height-to-wall distance of 0.635 cm produces the highest heat-transfer coefficients compared to the other heights. It also appears that the jet-to-jet interaction in the spanwise direction is stronger for this geometry than for the uniform diameter case.

Figure 8 presents the span-averaged heat-transfer coefficient distributions for each Reynolds number comparing the effect of jet height. The heat-transfer coefficients are plotted against actual distance in centimeters as in Fig. 6. For $Re = 2 \times 10^3$, the smallest height case (referred to as $Z/D = 1$) produces high heat-transfer coefficients for the first few rows. However, the heat-transfer coefficients deteriorate downstream with the region between the rows showing significantly lower heat-transfer coefficients. For the downstream rows of holes, the jet height appears to make very little difference to the peak heat-transfer coefficient values. The trends are similar for $Re = 6 \times 10^3$ and 10^3.

Comparison of Different Arrays

In this study, we have chosen to present all of the results in terms of heat-transfer coefficients and not Nusselt numbers because of the varying diameter effect. It is difficult to compare Nusselt numbers when the holes are varying in diameter from location to location.

Figure 9 compares the uniform diameter and varying diameter cases to results for square arrays obtained by Ekkad et al.[14] for $Re = 6 \times 10^3$. The holes are spaced four hole diameters apart in both spanwise and streamwise direction in their study with a hole diameter of 0.635 cm similar to the uniform diameter case. It is fairly evident that the varying diameter cases produce the highest heat-transfer coefficients among the three jet arrays except at $Z/D = 3$, where the uniform diameter case shows slightly higher heat-transfer coefficients for the upstream rows. The square arrays had only five rows, and so the crossflow effect was limited.

The degradation would have been significant if there were rows downstream of these five rows. The *UD* and the *VD* geometries are not truly comparable as the total flow area is varied between the arrays resulting in differences in hole jet velocities. However, basic pressure measurements show similar levels of pressure loss for both arrays. The *UD* array area is greater than the *VD* array area by a factor of almost two. It is automatically expected that the *UD* array will provide higher heat-transfer coefficients as a result of greater jet velocities for the upstream rows and lower heat-transfer coefficients for the downstream rows.

Comparison with Published Correlations

Kercher and Tabakoff[2] presented an impingement heat-transfer correlation based on a crossflow degradation coefficient. The impingement Nusselt number can be calculated from two functions ϕ_1 and ϕ_2 and a correction factor from the nondimensional jet-to-target pacing Z/D as

$$Nu_D \qquad \text{with crossflow} = \phi_1 \phi_2 Re_D^m Pr^{\frac{1}{3}} (Z/D)^{0.091}$$

where

$$\phi_1 = Nu_D Re_D^{-m} Pr^{-\frac{1}{3}}$$

for $Z/D = 1$ without crossflow, and

$$\phi_2 = \frac{Nu_{\text{with crossflow}}}{Nu_{\text{without crossflow}}}$$

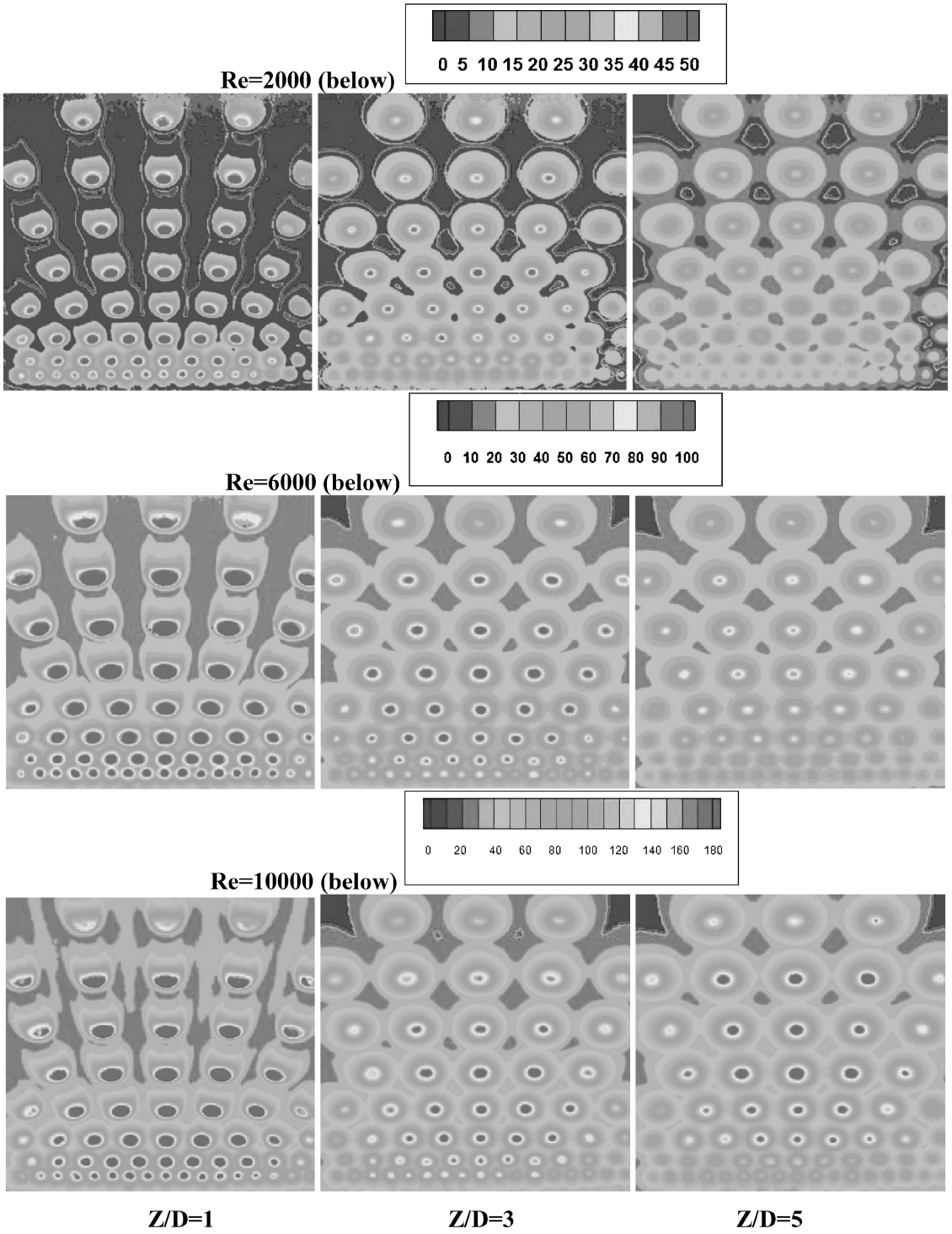

Fig. 7 Detailed Nusselt-number distributions for varying diameter jet plates.

The term ϕ_2 is called the degradation coefficient and is plotted against the term crossflow to jet flow mass flux ratio and the jet-to-target plate spacing. Figure 10 presents the variation of ϕ_2 vs $[G(X, I-1)/G(H, I)]|Z_n/D|$, where I represents the number of the impingement row. However, the measured range for their study for the x-axis value was up to1.7. In the present study, especially for variable arrays, the x-axis values as high as nine resulted in a need for extrapolation. If the curve is extended at the same degradation levels as for the earlier values, the values for ϕ_2 would produce negative Nusselt-number values. To avoid this problem, constant values of ϕ_2 are maintained for x-axis values greater than 2.0. This produced reasonable predictions for Nusselt numbers.

Florschuetz et al.[5] presented another correlation for jet-impingement heat transfer with crossflow effects. They arrived at a more detailed correlation given as

$$Nu = ARe_j^m \left\{1 - B[(Z/D)(G_c/G_j)]^n\right\} Pr^{\frac{1}{3}}$$

The values of A, m, B, and n depend on the pattern of the jet arrays. In the present study, each row was treated as an independent inline row, considering that they truly are not either staggered or inline patterns in the traditional sense. The values for the constants and exponents are obtained from the table provided in the paper. Using the preceding two correlations and the measured mass fluxes at

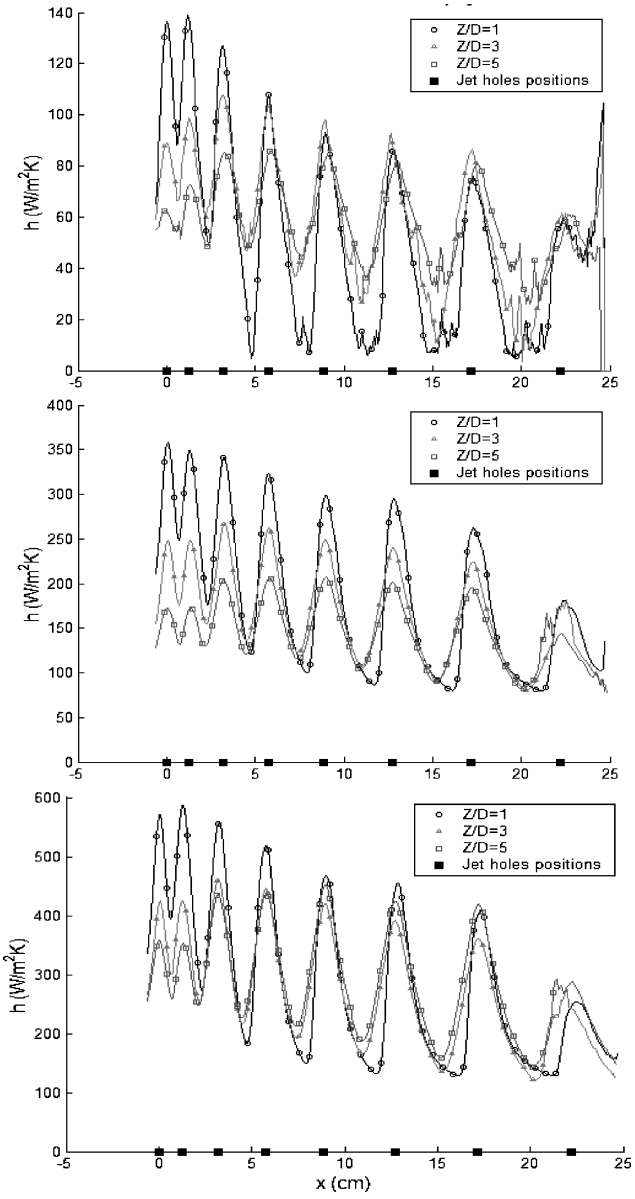

Fig. 8 Effect of jet height on span-averaged heat-transfer coefficients for varying diameter jet plate: top, $Re = 2 \times 10^3$; middle, $Re = 6 \times 10^3$; bottom, $Re = 10^3$.

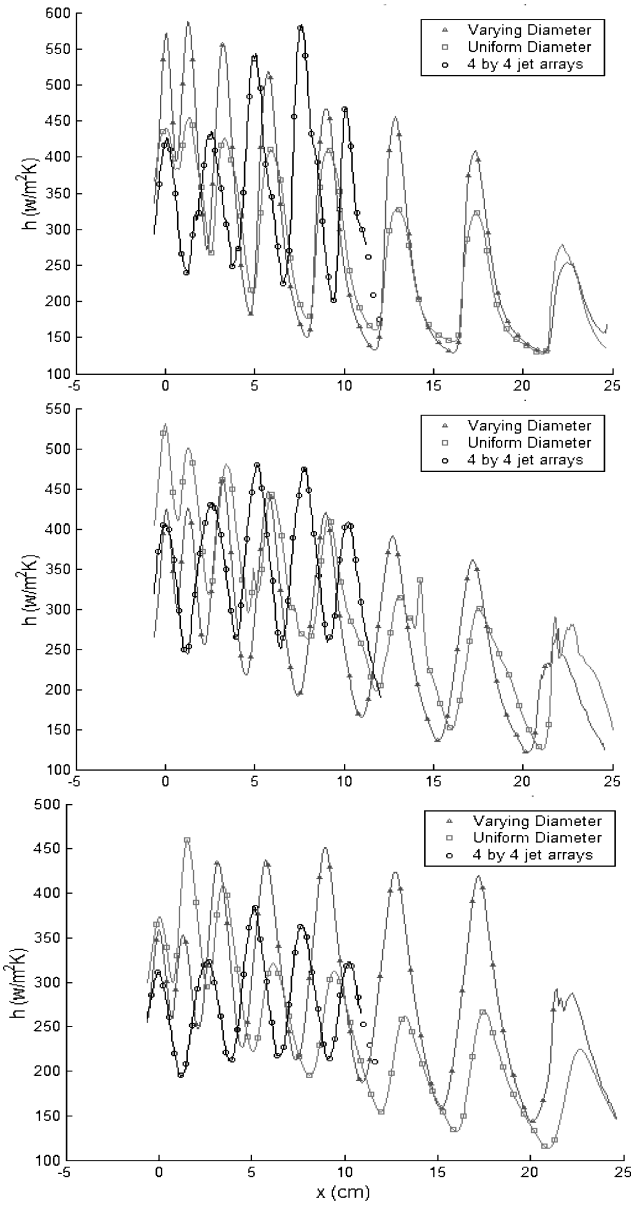

Fig. 9 Comparison of square array span-averaged heat-transfer coefficient distributions to stretched array distributions for $Re = 6 \times 10^3$ (top, $Z/D = 1$; middle, $Z/D = 3$; bottom, $Z/D = 5$).

each row, the local heat-transfer coefficients have been predicted for both uniform and variable diameter arrays. The local diameter of the jet hole and the spacings were used in the correlation to determine the local average heat-transfer coefficients for each row. Florschuetz et al.[5] correlation is valid for only $Re > 3 \times 10^3$, which can cause some errors in the predictions for $Re = 2 \times 10^3$ using their correlation. Both of the studies[2,5] presented correlations that provide regional-average or plate-average Nusselt numbers and not local distributions as obtained in the present study.

Figure 11 presents the regional-average heat-transfer coefficient comparisons for different Reynolds number for $Z/D = 3$ with the predictions from both the correlations. Both the correlations predict very high heat-transfer coefficients for the first row and show immediate degradation downstream for the rest of the rows. The degradation drops past the fifth row because the degradation constant ϕ_2 is held constant beyond this point. The first row is severely overpredicted as the correlation uses no crossflow at this point. In the present experiment, the first two rows produce identical levels of heat-transfer coefficients for all three jet heights and degrade downstream but not as rapidly as the correlation predicted values. Far downstream, it appears that the correlations and the experiments are

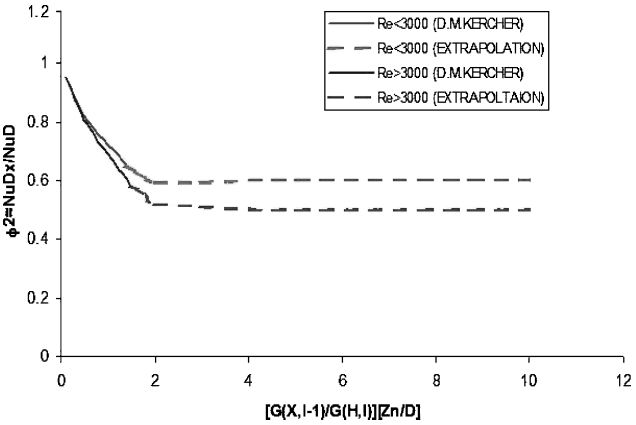

Fig. 10 Degradation of ϕ_2 coefficient as shown by Kercher and Tabakoff[2] and extrapolation.

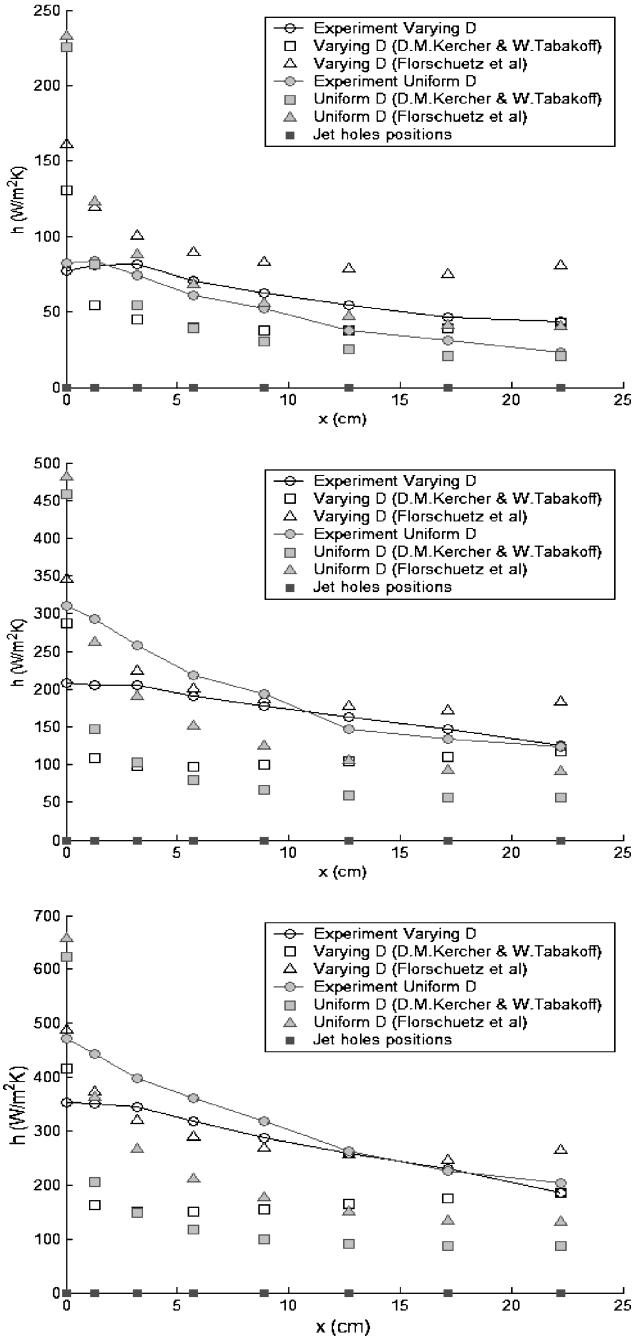

Fig. 11 Comparison of experimental data to published correlations: top, $Re = 2 \times 10^3$; middle, $Re = 6 \times 10^3$; bottom, $Re = 10^3$.

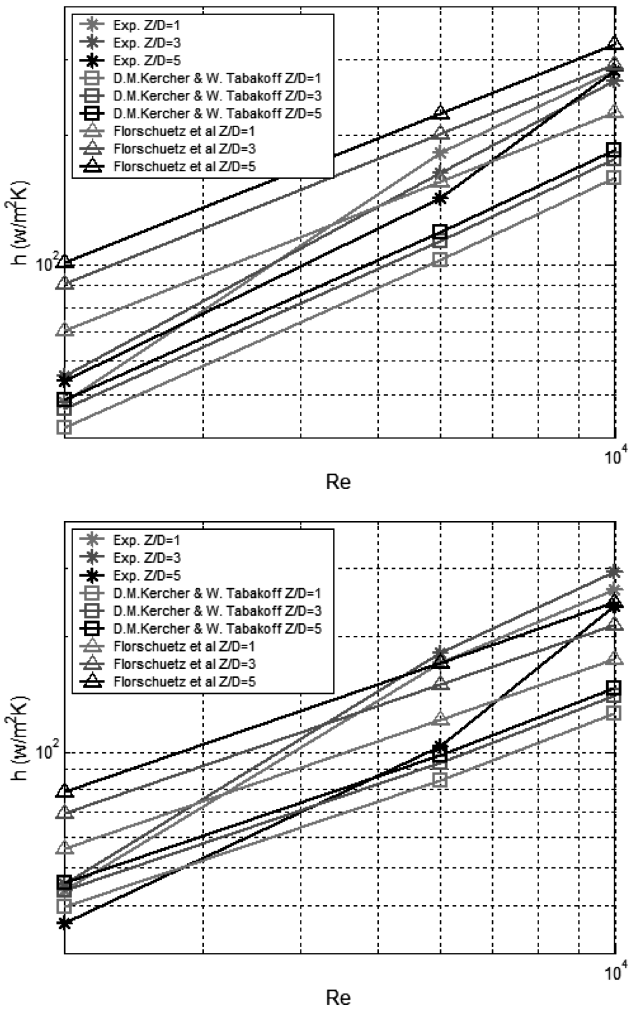

Fig. 12 Overall averaged heat-transfer coefficient comparisons for a) uniform diameter and b) varying diameter jet plates.

in good agreement. Kercher and Tabakoff[2] correlation consistently predicts values lower than that from Florschuetz et al.[5] correlation. In fact, the zero-crossflow first row has Kercher and Tabakoff[2] predicting closer values to the experiment. The crossflow effect is overpredicted for both the correlations resulting in lower heat-transfer coefficients than measured. Also, the lack of degradation values for large crossflow-to-jet flow ratios resulted in extrapolation, which can be causing the discrepancies in the predictions.

Figure 12 presents the overall averaged heat-transfer coefficients vs Reynolds number in a log-log plot for each of the jet heights. The overall averaged values obtained from the experiments lie between the predictions of both the correlations. The slope however is also different for the experimental data. The effect of jet height seems to be negligible for the varying diameter case. However, there are significant differences in the uniform diameter case with varying Z/D with $Z/D = 5$ providing the lowest heat-transfer coefficients. Florschuetz et al.[5] correlation predicts a much higher heat-transfer coefficient for the first row and a slightly lower heat-transfer coefficient for the rest of the rows resulting in an overall average heat-transfer coefficient higher than the experiment. Kercher and Tabakoff[2] correlation predicts experimental-level heat-transfer coefficients for the first row but much lower heat-transfer coefficients for the downstream rows resulting in lower overall average heat-transfer coefficients than the experiments.

Conclusions

Detailed heat-transfer coefficient distributions are presented for linearly stretched jet-impingement arrays. Two different arrays are investigated with uniform diameter holes through the array for one case and varying diameter holes at every row location for another case. The varying diameter and the uniform diameter holes are at the same physical locations resulting in different spanwise and streamwise spacing and also different jet heights at every row location for the varying holes case. Heat-transfer coefficients are typically higher for the varying holes on most of the test plate as expected, except for the first two rows where uniform holes produce higher heat-transfer coefficients as a result of increased jet flow. The varying diameter geometry also produces uniform flow rate through each of the rows. The predictions from the published correlations by Kercher and Tabakoff[2] and Florschuetz et al.[5] locally overpredict the effect of crossflow on heat transfer and underpredict the heat-transfer coefficients when under strong crossflow effects. The correlations also overpredict the heat-transfer coefficients at the first row where crossflow is nonexistent. The overall average results show that the experimental results lie between the predictions of the two correlations, and also the slope of the line with Reynolds number is

different than both the correlations. This might be strongly evident at higher Reynolds numbers than the ones investigated in this study. In conclusion, there is a need to investigate jet-impingement heat transfer for extremely strong crossflow condition as the existing correlations do not cover the range. In this study, an extrapolation that seems inadequate and incorrect was also used.

Acknowledgments

The authors acknowledge the support from the project funded by the Louisiana Board of Regents through the NASA-LaSPACE REA under contract from NASA/LEQSF. The program manager is John Wefel. Acknowledgments are also given to Hasan Nasir for help with the initial design and experimental setup.

References

[1]Chupp, R. E., Helms, H. E., McFadden, P. W., and Brown, T. R., "Evaluation of Internal Heat Transfer Coefficients for Impingement Cooled Turbine Blades," *Journal of Aircraft*, Vol. 6, No. 1, 1969, pp. 203–208; also AIAA Paper 6-564.

[2]Kercher, D. M., and Tabakoff, W., "Heat Transfer by a Square Array of Round Air Jets Impinging Perpendicular to a Flat Surface Including the Effect of Spent Air," *Journal of Engineering and Power*, Vol. 92, No. 1, 1970, pp. 73–82.

[3]Chance, J. L., "Experimental Investigation of Air Impingement Heat Transfer Under an Array of Round Jets," *TAPPI*, Vol. 57, No. 1, 1974, pp. 108–112.

[4]Florschuetz, L. W., Berry, R. A., and Metzger, D. E., "Periodic Streamwise Variation of Heat Transfer Coefficients for Inline and Staggered Arrays of Circular Jets with Crossflow of Spent Air," *Journal of Heat Transfer*, Vol. 102, No. 1, 1980, pp. 132–137.

[5]Florschuetz, L. W., Truman, C. R., and Metzger, D. E., "Streamwise Flow and Heat Transfer Distribution for Jet Impingement with Crossflow," *Journal of Heat Transfer*, Vol. 103, No. 2, 1981, pp. 337–342.

[6]Behbahani, A. I., and Goldstein, R. J., "Local Heat Transfer to Staggered Arrays of Impinging Circular Air Jets," *Journal of Engineering and Power*, Vol. 105, No. 3, 1983, pp. 354–360.

[7]Florschuetz, L. W., Metzger, D. E., and Su, C. C., "Heat Transfer Characteristics for Jet Array Impingement with Initial Crossflow," *Journal of Heat Transfer*, Vol. 106, No. 1, 1984, pp. 34–41.

[8]Downs, S. J., and James, E. H., "Jet Impingement Heat Transfer—A Literature Survey," American Society of Mechanical Engineers, Paper 87-HT-35, Nov. 1987.

[9]Huber, A. M., and Viskanta, R., "Comparison of Convective Heat Transfer to Perimeter and Center Jet in a Confined, Impinging Array of Axisymmetric Air Jets," *International Journal of Heat and Mass Transfer*, Vol. 37, No. 18, 1994, pp. 3025–3030.

[10]Huber, A. M., and Viskanta, R., "Effect of Jet-Jet Spacing on Convective Heat Transfer to Confined, Impinging Arrays of Axisymmetric Air Jets," *International Journal of Heat and Mass Transfer*, Vol. 37, No. 18, 1994, pp. 2859–2869.

[11]Van Treuren, K. W., Wang, Z., Ireland, P. T., and Jones, T. V., "Detailed Measurements of Local Heat Transfer Coefficient and Adiabatic Wall Temperature Beneath an Array of Impingement Jets," *Journal of Turbomachinery*, Vol. 116, No. 2, 1994, pp. 369–374.

[12]Huang, Y., Ekkad, S. V., and Han, J. C., "Local Heat Transfer Coefficient Distribution Under an Array of Impinging Jets Using a Transient Liquid Crystal Technique," *Journal of Thermophysics and Heat Transfer*, Vol. 12, No. 1, 1998, pp. 73–79.

[13]Bailey, J. C., and Bunker, R. S., "Local Heat Transfer and Flow Distributions for Impinging Jet Arrays of Dense and Sparse Extent," American Society of Mechanical Engineers, Paper GT-2002-30473, June 2002.

[14]Ekkad, S. V., Gao, L., and Hebert, R. T., "Effect of Jet-to-Jet Spacing in Impingement Arrays on Heat Transfer," American Society of Mechanical Engineers, Paper IMECE2002-32108, Nov. 2002.

[15]Ekkad, S. V., and Han, J. C., "A Transient Liquid Crystal Thermography Technique for Gas Turbine Heat Transfer Measurements," *Measurement Science and Technology*, Vol. 11, July 2000, pp. 957–968.

[16]Kline, S. J., and McClintock, F. A., "Describing Uncertainties in Single Sample Experiments," *Mechanical Engineering*, Vol. 75, No. 1, 1953, pp. 3–8.